LEACHING THERMODYNAMICS AND KINETICS OF OIL SHALE WASTE KEY COMPONENTS

KADRIANN TAMM[*], PRIIT KALLASTE, MAI UIBU, JUHA KALLAS, OLGA VELTS-JÄNES, REIN KUUSIK

Laboratory of Inorganic Materials, Tallinn University of Technology, Ehitajate tee 5, 19086 Tallinn, Estonia

Abstract. *Estonia is strongly dependent on locally mined oil shale which is the main fuel for power and oil production. Vast amounts of solid wastes are formed from circulating fluidized bed (CFB), pulverized firing (PF), and solid heat carrier (SHC) technologies, and are currently wet deposited in open-air fields. Both the utilization of newly produced ash and the management of historical deposits require an accurate thermodynamic modelling of complex mixtures. The authors investigated the leaching of the main water-soluble Ca-compounds from three types of oil shale mineral waste and developed a kinetic model that was used to determine the equilibrium constants and kinetic parameters of dissolution reactions for all three ash-water systems over a wide range of solid-to-liquid (S/L) ratio. For this, we prepared binary $(Ca(OH)_2\text{-}CaSO_4 \cdot 2H_2O\text{-}H_2O)$ and ternary $(Ca(OH)_2\text{-}CaSO_4 \cdot 2H_2O\text{-}CaS\text{-}H_2O)$ model systems that reflect the composition of the three different ashes, and measured the kinetics of dissolution for both the model systems and industrial ash. Thermodynamic calculations were performed using HsC Chemistry® 7.1 and Aspen Plus V8.6 while the leaching kinetics was simulated employing the MODEST 6.1 software package. By comparing the results obtained for our model systems with those obtained for industrial oil shale ash-water systems the authors were able to both verify that the model results coincided to a satisfactory degree with simulation data, and also propose models that may aid one to design shale ash processing technologies.*

Keywords: *oil shale ash, HsC chemistry, calcium compounds, sulfur compounds.*

1. Introduction

About 60% of Estonia's fuel balance is covered by local low-grade oil shale (OS), which is mainly used to produce heat, power, and shale oil. Oil shale

---

[*] Corresponding author: e-mail *kadriann.tamm@ttu.ee*

processing generates vast amounts of solid waste of varying composition depending on both the composition of raw OS and processing conditions [1]. 45–48% of OS dry matter remains as solid waste [2].

The oil shale ash (OSA) from thermal power plants contains mainly free lime (CaO_{free}), Ca-sulfate, secondary Ca(Mg)-silicate minerals, and an amorphous Al-Si glass phase [3–5]. Both the high temperatures and thermal processing conditions as well as combustion conditions (> 750 °C, residence time, combustion regime – pulverized firing (PF) or circulating fluidized bed (CFB) combustion) ensure that all of the organic matter (mainly kerogen) in OS (up to 65% [6]) is burnt out [1].

Gaseous heat carrier (GHC) and solid heat carrier (SHC) retorts are used to produce shale oil. In the SHC process, OS is heated in the absence of oxygen by continuously mixing the combusted retorting residue at about 800 °C [7, 8]. During the last stage of the process, the retorting residue is combusted in an aero furnace at temperatures up to 950 °C. The resulting solid residue consists mainly of calcite, quartz, K-feldspar, and dolomite, with only trace amounts of CaO_{free}. The composition of this residue is similar to that of ash produced in the circulating fluidized bed furnaces at thermal power plants, but contains up to a few percent of unburnt organic matter due to the short residence time in the combustion stage [8, 9].

Eesti Energia, Estonia's major power company, deposited 7.9 Mt of OSA and emitted 12.8 Mt of CO_2 in 2014 [10]. At the same time, the largest OS retorting company, VKG OIL Ltd., processed 2.9 Mt of OS and produced 433,000 t of shale oil [11]. In 2013, VKG processed 2.8 Mt of OS and generated approximately 1.48 Mt of ash and about 0.9 MT of semicoke type retorting waste [12]. The safe disposal and/or reuse of OS ash waste, together with atmospheric emissions (CO_2, SO_2, NO_x, etc.), are among the most serious environmental problems in Estonia.

Today, about 90% of oil shale ash is wet deposited in ash fields near the power plants. Only a small percentage of OSA is utilized, either in the building materials industry, in agriculture as a liming agent, or in road construction [5]. OSA is classified as a "hazardous waste" mainly due to the high alkalinity of leachates (pH values 12–13), contributed by the dissolution of free lime (up to 30 wt%). However, this property makes OSA (or OSA leachates) an attractive material for CO_2 mineralization [13, 14] or producing precipitated calcium carbonate (PCC) [15, 16]. Currently, the lack of kinetic process data, including that characterizing leaching, impedes the implementation of more effective waste valorization and environmental pollution control methods.

The current study investigates the dissolution mechanisms of OS mineral waste. In order to better understand the behavior and impact of the waste's key components on the leaching process, both binary and ternary model systems were prepared to match the composition of OS processing ashes and investigated for comparison. The aim of the study was to elaborate the leaching equilibriums and dynamics of the main water-soluble Ca-compounds of

OSAs, as a basis for mathematical models, which simulate the processes of leaching. The results provide a basis for designing a complete OSA neutralization and/or carbonation process.

2. Materials and methods

2.1. Characterization of materials

Three types of ash were used as Ca-rich raw materials. The circulating fluidized bed ash mixture (taken from the common silo) and pulverized firing cyclone ash were collected from Eesti Power Plant of Narva Power Plants in 2011. The SHC ash was collected in 2012 from the final residue resulting from the shale oil production process at the VKG retorting plant.

Each ash sample was analyzed using both X-ray fluorescence spectroscopy (XRF, Rigaku Primus II) and quantitative X-ray diffraction (XRD, Bruker D8 Advanced) methods at the Institute of Geology, University of Tartu (UT). The contents of free lime (CaO_{free}) (ethylene glycol method) [17], different forms of sulfur (sulfate and sulfide) [18], total carbon (TC) and inorganic carbon (TIC) (Electra CS - 580 Carbon/ Sulfur Determinator) were determined. The BET specific surface area (SSA) was determined using a Kelvin 1042 sorptometer. The chemical and mineral composition as weight percentages together with the SSA values of the three ashes are provided in Table 1.

Of the three ashes, PF ash is characterized by the highest free lime content. The sulfates in CFB ash are present mainly in the form of anhydrite ($CaSO_4$), which in water systems crystallizes into gypsum ($CaSO_4 \cdot 2H_2O$). In both the CFB and PF ashes the content of sulfides (mainly CaS) is relatively low. SHC ash is characterized by high sulfide content. This ash also contains organic matter with a chemical oxygen demand of 99 ± 10 mg/L as measured according to the method described in [19], which is present because the residence time in the final burner at the oil factory is insufficient to ensure complete pyrolysis. The presence of organics also causes the high porosity and surface area of the retorted ashes [20]. The SSA of both CFB and SHC ashes is more than ten times that of PF ash (Table 1). Under ambient conditions the sulfides from each of these ashes can be emitted into the atmosphere as gaseous H_2S, generating atmospheric pollution. Sulfides, which remain in the aqueous phase, may also induce toxic effects depending on the pH of the suspension [21].

Table 1. The composition and SSA of OS ashes in wt% and m$^2 \cdot$g^{-1}

Chemical composition	CFB	PF	SHC
CaO$_{free}$	12.31	22.37	1.89
SO$_4^{2-}$	7.90	5.24	1.82
S^{2-}	0.64	0.064	1.22
TC	3.03	0.30	7.82
TIC	3.03	0.30	6.45
TOC	0	0	1.37
Mineral composition	CFB	PF	SHC
Quartz (SiO$_2$)	11.40	4.40	14.10
K-feldspar (KAlSiO$_4$)	10.20	3.90	12.70
Calcite (CaCO$_3$)	27.70	3.30	29.40
Lime (CaO)	9.30	28.30	3.00
Portlandite (Ca(OH)$_2$)	1.10	0	–
Anhydrite (CaSO$_4$)	10.10	8.60	0.70
Periclase (MgO)	2.70	5.10	8.70
Dolomite (CaMg(CO$_3$)$_2$)	1.40	0	10.00
Wollastonite (CaSiO$_3$)	1.20	3.70	1.90
Belite (Ca$_2$SiO$_4$)	6.70	24.00	–
Alite (Ca$_3$SiO$_5$)	1.40	0	–
Merwinite (Ca$_3$Mg(SiO$_4$)$_2$)	0.80	6.30	1.30
Melilite ((CaMg)$_2$(MgAl)(SiAl)$_3$O$_7$)	2.50	8.20	1.20
Brownmillerite (4CaO·Al$_2$O$_3$·Fe$_2$O$_3$)	1.30	2.40	2.20
Hematite/magnetite (Fe$_2$O$_3$/Fe$_3$O$_4$)	2.20	1.30	1.60
Jasmundite (Ca$_{11}$(SiO$_4$)$_4$O$_2$S)	1.70	0	–
Calcium ferrite (2CaO·Fe$_2$O)	1.30	0	–
Yeelimite (Ca$_4$Al$_6$(SO$_4$)O$_{12}$)	0.60	0	–
Albite (NaAlSi$_3$O$_8$)	–	–	1.60
Rankinite (Ca$_3$Si$_2$O$_7$)	–	–	0.90
Illite (K$_y$Al$_4$(Si$_{8-y}$,Al$_y$)O$_{20}$(OH)$_4$)	6.40	0	3.40
Ca-Al pyroxene (CaAl$_2$SiO$_6$)	2.50	8.20	1.20
Physical characteristic	CFB	PF	SHC
SSA, m$^2 \cdot$g^{-1}	6.30	0.40	7.44

2.2. Experimental procedure

All experiments with CFB, PF and SHC ash-water systems as well as the corresponding binary (Ca(OH)$_2$-CaSO$_4 \cdot$2H$_2$O-H$_2$O) and ternary (Ca(OH)$_2$-CaSO$_4 \cdot$2H$_2$O-CaS-H$_2$O) model systems were performed at room temperature and atmospheric pressure. The selected ash-to-water ratios ranged from 0.004–0.200 and were selected based on the results of previous studies [22], and the parameters (ash-to-water ratio of 1.20) used in the hydrotransport of OSA. Model binary and ternary ash mixtures were made of pure Ca(OH)$_2$ (BDH, 95% purity), CaSO$_4 \cdot$2H$_2$O (lach:ner, 99% purity), and CaS (Alfa Aeser, 99.9% purity) as sources of Ca^{2+}, SO$_4^{2-}$ and S^{2-} ions. For a comparative study the proportions of components in model systems were chosen according to their content in the respective OSAs.

To achieve an equilibrium state, the systems under study were kept in closed centrifuge tubes for 3 h in an overhead shaker (GFL 3025) at 45 rpm

throughout the experiment. The suspensions were prepared in 50 mL tubes sealed with airtight caps beforehand. The pH (MT SevenGo pH) and electrical conductivity of the suspensions (MT SevenGo Duo Pro) were measured immediately after a 3 h experiment. The dissolution kinetics of these systems was determined in a batch reactor. For this, 0.750 L of deionized water (conductivity 0.05 μS/cm) was poured into a 1 L Lara Controlled Lab Reactor. The stirrer was set to revolve at 250 rpm and a thermostat (Huber Unistat 405) kept the entire system at 25 °C in the course of the experiment. A pause control program momentarily halted the stirring while the solid phase was quickly added to the system using a funnel. Each suspension was maintained as a closed system for one hour. The conductivity (Mettler Toledo SevenGO Duo Pro with LabX software), pH (Knick Portamess 913 pH; Hamilton Polylyte Plus VP360 pH-meter sensor) and temperature of the solution were continuously monitored during the experiment. The resulting suspensions were then filtered using a vacuum filter (Munktell filter paper, 100 g/m^2). The contents of calcium (Ca^{2+} ions), total reduced sulfur, and alkalinity (OH$^-$, CO$_3^{2-}$ and HCO$_3^-$ ions) were determined using titration methods, the ISO-6058:1984 method [23], iodometric titration [24], and the ISO-9963-1:1994(E) method [25], respectively. The content of total sulfide was determined as the sum of dissolved sulfide (S^{2-}, HS$^-$, H$_2$S) and SO$_4^{2-}$ ions, using a Lovibond Spectro Direct spectrometer, and DPD/Catalyst and barium sulfate turbidity methods, respectively.

2.3. Modeling software

The equilibrium calculations were carried out using thermodynamic programs based on the Gibbs free energy minimization technique. The Aspen Plus RGibbs reactor model, which employs the ELECNRTL model together with the Aspen Plus V8.6 default databases, and the HsC Chemistry$^{®}$ 7.1 program were applied to both determine the composition of each phase and predict the equilibrium composition of ternary systems according to the composition of the three ashes (CFB, PF, SHC). The equilibrium composition of the real CFB ash-water system was also investigated using the HsC program.

2.4. Process chemistry

Equations (1)–(7) represent a simplified dissociation (equilibriums (1)–(3) and (6)–(7)) for OSA and ternary (Ca(OH)$_2$-CaSO$_4$·2H$_2$O-CaS-H$_2$O) model systems:

$$[CaS] \underset{k_{12}}{\overset{k_{11}}{\rightleftharpoons}} [Ca^{2+}] + [S^{2-}] \qquad\qquad K_{eq1}, \qquad (1)$$

$$[S^{2-}] + [H_2O] \underset{k_{22}}{\overset{k_{21}}{\rightleftharpoons}} [HS^-] + [OH^-] \qquad\qquad K_{eq2}, \qquad (2)$$

$$[\text{HS}^-] + [\text{H}_2\text{O}] \underset{k_{32}}{\overset{k_{31}}{\rightleftharpoons}} [\text{H}_2\text{S}] + [\text{OH}^-] \qquad \text{K}_{\text{eq3,}} \qquad (3)$$

$$2[\text{HS}^-] + 2[\text{O}_2] \overset{k_{41}}{\rightarrow} [\text{S}_2\text{O}_3^{2-}] + [\text{H}_2\text{O}], \qquad (4)$$

$$[\text{HS}^-] + 2[\text{O}_2] \overset{k_{51}}{\rightarrow} [\text{SO}_4^{2-}] + [\text{H}^+], \qquad (5)$$

$$[\text{Ca(OH)}_2] \underset{k_{62}}{\overset{k_{61}}{\rightleftharpoons}} [\text{Ca}^{2+}] + 2[\text{OH}^-] \qquad \text{K}_{\text{eq6,}} \qquad (6)$$

$$[\text{CaSO}_4] \underset{k_{72}}{\overset{k_{71}}{\rightleftharpoons}} [\text{Ca}^{2+}] + [\text{SO}_4^{2-}] \qquad \text{K}_{\text{eq7,}} \qquad (7)$$
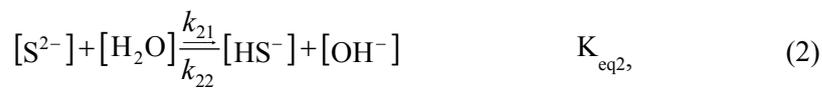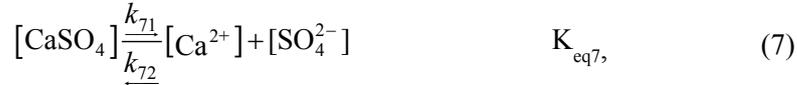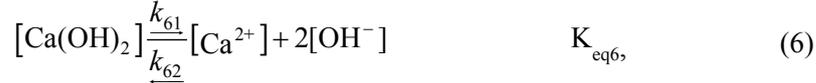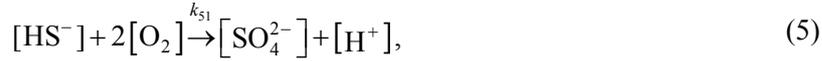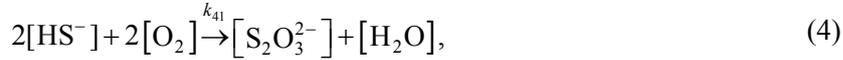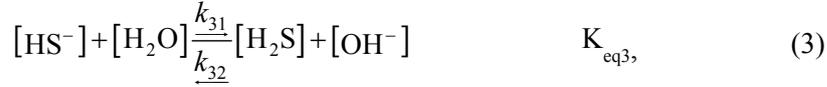
where K_{eq1}–K_{eq3} and K_{eq6}–K_{eq7} are the equilibrium constants expressed on a molar basis, k_{11}–k_{71} (in the numerator) are the forward reaction rate constants, and k_{12}–k_{72} (in the denominator) are the reverse reaction rate constants, s^{-1}.

The Ca(OH)_2 dissolution mechanism is presented as a one-step reaction system for a more universal approach [26]. The formation of gaseous H_2S is not included in the proposed model. As a more complex approach, a two-step reaction system for lime dissolution ($\text{Ca(OH)}_2 \leftrightarrow \text{CaOH}^+ + \text{OH}^-$; $\text{CaOH}^+ \leftrightarrow \text{Ca}^{2+} + \text{OH}^-$) and further hydrolysis of sulfide are included in the Aspen Plus ternary and HsC Chemistry® (also the formation of gaseous H_2S) models (in all OSA based ternary systems and the CFB ash system).

3. Results and discussion

The following section will discuss the results of thermodynamic and kinetic calculations for ternary model systems and the solubility results for the experimentally measured binary and ternary models as well as OS ash-water systems.

3.1. Simulation approach

The thermodynamic calculations show that at the equilibrium state the unstable compounds are bound to the steady phase (Fig. 1). Its final composition indicates mineral changes to have taken place in OSA after leaching for an unlimited period of time. At equilibrium, quartz does not occur, and therefore, Ca-silicate minerals dominate, oxides are present as their hydrated forms, also gypsum is formed from the original anhydrate.

Both the binary and ternary tests were carried out using Ca(OH)_2 and $\text{CaSO}_4 \cdot \text{H}_2\text{O}$ as the main Ca^{2+} and SO_4^{2-} ion sources in OS ash-water systems. Thermodynamic calculations show the results obtained using Aspen Plus V6.8 and HsC Chemistry® 7.1 to coincide (Fig. 2).
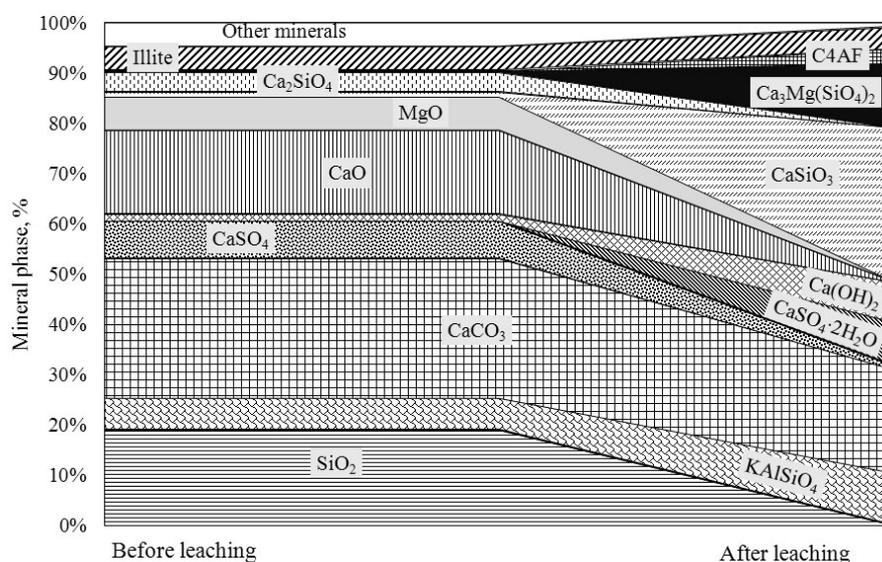
Fig. 1. The composition of theoretical CFB ash (S/L 1:10) and mineral changes in it during the leaching process (HsC Chemistry® 7.1).
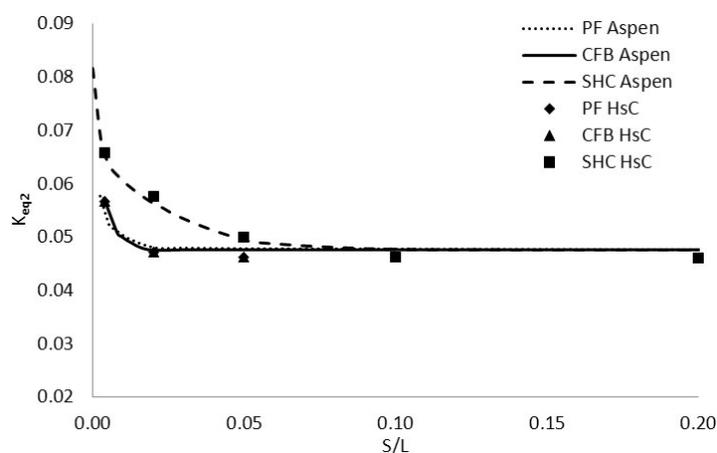
Fig. 2. Apparent equilibrium of ternary model systems (Aspen Plus V8.6 and HsC Chemistry® 7.1 simulation).

The simulation results revealed that the equilibrium state of the ion distribution was achieved for the most oversaturated systems (S/L ratio ≥ 0.1). Both the CFB and PF ash-water systems had similar equilibrium concentrations of the observed species.

The equilibrium constant K_{eq2} for Equation (2) was calculated from the simulated equilibrium composition for the OS ash-water model systems (Fig. 2). K_{eq2} was calculated from the results of both the Aspen Plus V8.6 and HsC Chemistry® 7.1 simulations, which coincided, and this value was

used to determine the distribution of sulfide forms in both the model and real OS ash-water systems.

To compare experimental results, the sum of Ca^{2+} (Ca^{2+} + $CaOH^+$) and OH^- (OH^- + $CaOH^+$) ions, and $S_{sulfide}$ (S^{2-} + HS^- + H_2S) were used to determine the equilibrium constants (K_{eq1}, K_{eq6} and K_{eq7}) for Equations (1), (6) and (7).

The equilibrium constant K_{eq3} (reported as 1×10^{-7} in [27, 28]) for Equation (3) was calculated from the equilibrium concentration of pure CaS.

3.2. Solubility results

By varying the content of the model components of OS ash-water systems according to the ash-to-water ratios from 0.004 to 0.200 and allowing the batch experiments to achieve equilibrium, we were able to determine the system pH, conductivity, and the concentration of the main ion species (Ca^{2+}, SO_4^{2-}, $S_{sulfide}$) in the liquid phase. The leaching equilibrium of the three types of ashes and the corresponding ternary model systems are shown in Figure 3. The average pH and conductivity (E) were determined based on the experimentally measured values of the equilibrium state model and ash-water systems.

The pH values (12.31–12.66) of saturated binary and ternary systems coincided with those of real OS ash-water systems. The highest pH values occurred in the PF ash based system because this ash contained the highest amount of initial free lime.

The conductivity values determined at saturation for CFB and SHC ash model systems were higher (up to 9.97 mS/cm) than that for the PF ash model system, which tended to stabilize at lower values (up to 9.58 mS/cm). This indicates that the high initial CaS content has a stronger influence on the conductivity of the ions that remain in the aqueous phase than the other components. In real OS ash-water systems, the lowest conductivity values occurred in the SHC ash-water system (10.35 mS/cm) while the PF ash-water system had the highest conductivity (up to 12.25 mS/cm), which in this case was driven by the higher content of free lime and Ca-silicate phases.

At saturation, both Ca^{2+} and SO_4^{2-} ions were present in similar concentrations in all model systems (0.033–0.035 and 0.014–0.015 mol/L, respectively). At the same time, the respective values were slightly higher in the ternary model systems due to the dissolution of CaS (Eqs. (1)–(3)) and the oxidation of sulfide ions to intermediate forms (Eq. (4)) and sulfate (Eq. (5)). Due to the similarity in leaching mechanism between the binary and ternary model systems, the small ion concentration variations of about 0.001 mol/L can be neglected, hence, the results of binary model systems are not shown in Figure 3. The concentrations of Ca^{2+} and SO_4^{2-} ions (ca 0.034 and 0.009 mol/L, respectively) were lower in the SHC ash-water system than in both the CFB and PF ash-water systems (ca 0.040 and 0.016 mol/L, respectively). The latter is related to the original composition of the ashes (Table 1). In the ash of the SHC system, the content of leachable SO_4^{2-} and Ca^{2+} ions was lower than in PF and CFB ashes.
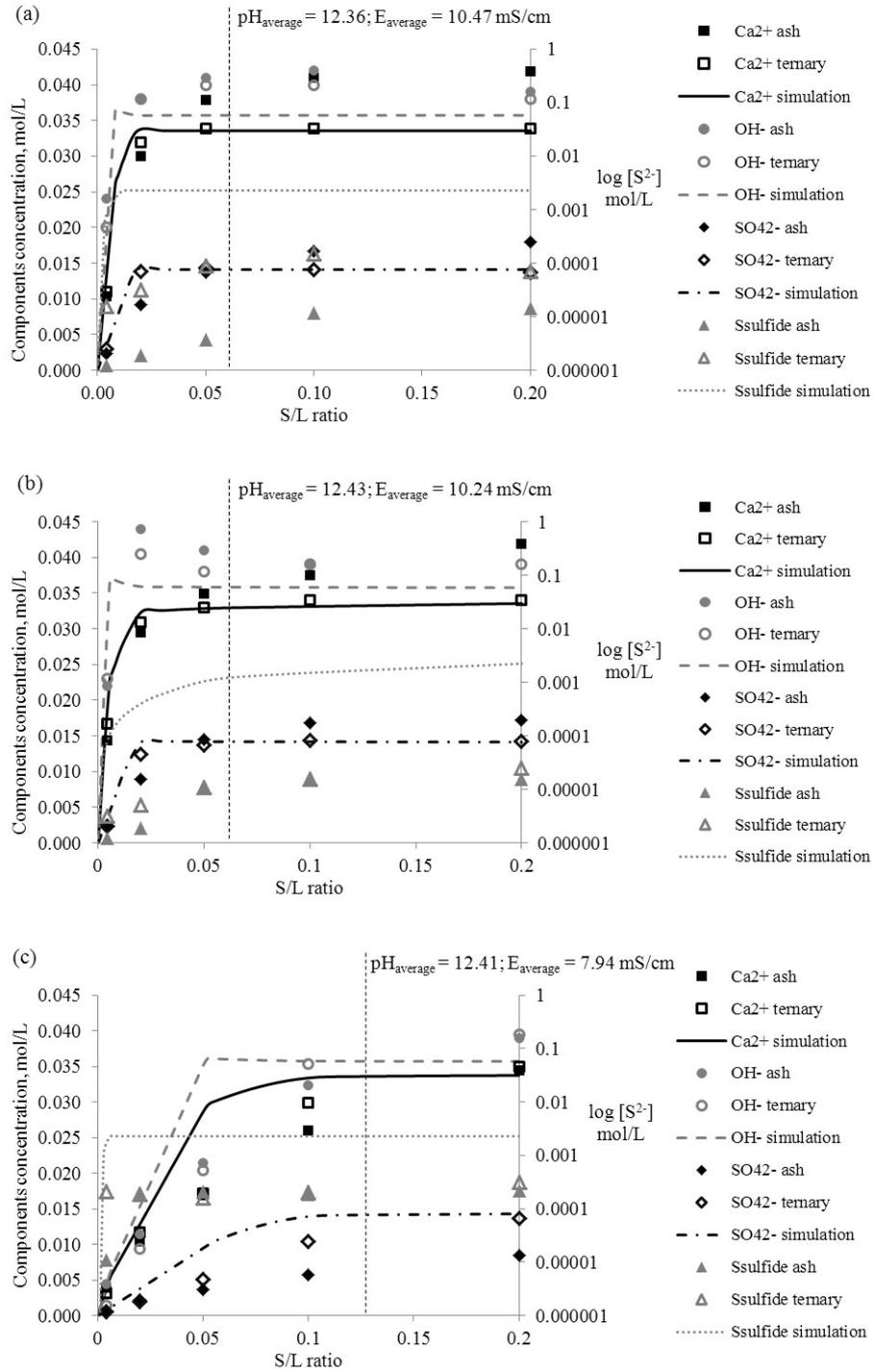
Fig. 3. Experimental vs simulation dissolution data for OSA from: (a) CFB; (b) PF; (c) SHC.

The SHC ash-water system with the highest initial CaS content can also be clearly distinguished by the leaching of sulfides. The total sulfide concentration in the SHC ternary model system was up to 5.6×10^{-4} mol/L, which is notably higher compared with both the CFB and PF ternary model systems (7.9×10^{-5} and 2.1×10^{-5} mol/L, respectively). Total sulfide concentrations in the leachates of CFB and PF ash-water systems remained at 1.5×10^{-5} mol/L, and were up to 20 times that in the SHC ash-water system, which stayed at 2.2×10^{-4} mol/L (the equilibrium concentration was not reached under our experimental conditions). Though there was no remarkable difference in initial CaS content between the ashes compared, the leaching of CaS was favored in the SHC ash-water system.

The parameters of the ternary ash-water model and real OS ash-water systems were well comparable. The small differences observed were caused by other water-soluble OS ash components (Table 1). Consequently, the OS ash leaching scheme can be modeled using our ternary model system.

The predicted dissociation results for the OS ash-water systems (Eqs. (1)–(7)) were compared with the experimental data (Fig. 3). The relatively small differences in the measured and predicted data confirm the ability of the proposed model to describe accurately the dissolution process of OS ash-water systems. The variability in sulfide concentrations is largely due to uncertainties in the experimentally determined solubility of pure CaS. In our previous work [29], the CaS solubility was determined after three hours of dissolution under both an inert atmosphere (2.29×10^{-3} mol/L) and atmospheric conditions (2.74×10^{-3} mol/L). The experimental results show a

Fig. 4. Relationship between Ca^{2+} ion concentration and conductivity in ternary model and OSA based water systems.

strong relationship between the Ca^{2+} ion concentration and conductivity (E) of the solution for all of the OS ash-water systems, including the ternary $(Ca(OH)_2$-$CaSO_4 \cdot 2H_2O$-$CaS)$ model ($R^2 = 0.986$), and CFB, PF and SHC ash-water systems (Fig. 4).

Including the experimentally determined pH values of the solutions as a main parameter in addition to E did not improve significantly the correlation coefficient, therefore the correlation is expressed as the following averaged equation (8) ($R^2 = 0.982$):

$$[Ca^{2+}] = 0.003375 \cdot E, \tag{8}$$

where Ca^{2+} is the concentration of calcium ions expressed in mol/L and E is the system conductivity in mS/cm.

The earlier studies have shown that Ca^{2+} and SO_4^{2-} are the main leachable ions in OS ash leachates, the leachability of K^+ is one order of magnitude lower and Na^+, Al^{3+} and Mg^{2+} have been detected at minor levels [1, 30]. Also, the presence of other anions (Cl^-, S^{2-}, SO_3^{2-}, $S_2O_3^{2-}$ and PO_4^{3-}) in small concentrations has been detected [31–33]. However, the sum of Ca^{2+}, SO_4^{2-} and OH^- ions corresponds to 90–95% of the electroneutrality condition. Based on optimal linear approximation (Eq. (8)), the concentration of Ca^{2+} ions can be determined for OS ash-water systems from conductivity measurements and compared with the predictions from the kinetic model. This approach may aid in optimizing an industrial PCC process using OS ash-water systems as a feedstock.

The equilibrium constants were calculated from the experimental data using the thermodynamic model and are presented as average values in Table 2. These results indicate that the experimental and predicted values of K_{eq6} and K_{eq7} ($K_{eq6} = 6.37 \times 10^{-5}$, $K_{eq7} = 5.21 \times 10^{-4}$ and $K_{eq6} = 4.28 \times 10^{-5}$, $K_{eq7} = 4.73 \times 10^{-4}$, respectively) agree for the ternary model systems quite well. Comparison of the results of ternary model (experimental and simulated) and OS ash-water systems shows the K_{eq6} and K_{eq7} values for real OS ash-water systems to be higher due to the presence of additional ash components that could provide Ca^{2+} and SO_4^{2-} ions into the solution. The value of K_{eq6} (5.24×10^{-5}) reveals the largest discrepancy from the result of

Table 2. Equilibrium constants of the systems under study

K_{eq} / OSA, mol/L	Experimental				Simulated (Aspen ternary)			
	K_{eq1}	K_{eq2}	K_{eq6}	K_{eq7}	K_{eq1}	K_{eq2}	K_{eq6}	K_{eq7}
CFB system	4.05×10^{-7}	4.61×10^{-2}	6.66×10^{-5}	6.52×10^{-4}	7.68×10^{-5}	4.76×10^{-2}	4.28×10^{-5}	4.73×10^{-4}
PF system	5.36×10^{-7}	4.61×10^{-2}	7.21×10^{-5}	6.18×10^{-4}				
SHC system	7.52×10^{-6}	4.61×10^{-2}	5.24×10^{-5}	2.93×10^{-4}				

the SHC model system (5.45×10^{-5}), which indicates that in SHC ash, the balance between calcium and hydroxide ions affects the concentration of all the main components. The value of K_{eq7} found for the ternary model matches better with that established for the CFB and PF ash-water systems because the concentration of SO_4^{2-} ions does not reach equilibrium in the real SHC ash-water system. The oxidation reactions (Eqs. (4) and (5)) are expressed as unidirectional because the backward reactions do not occur during the initial combustion processes. However, oxidation in aqueous suspensions takes place as long as sulfide ions are present as "combustible matter". Considering this, our 3 h experiments do not reflect the endpoint of sulfide oxidation in the suspension. The values of K_{eq1} for OS ash-water and ternary model systems are also comparable, agreeing with that for the PF ash-water system that has low sulfide content. However, these values significantly differ from the respective simulation figures because our model currently takes into consideration the solubility of CaS in pure water. Consequently, the $Ca(OH)_2$-$CaSO_4 \cdot H_2O$-CaS-H_2O model system should be adjusted according to the new experimental data.

Although the ashes of the three types of OS ash-water systems differ in both chemical and physical structure (Table 1) but yet remain comparable with the results for our model ash, we can state that the proposed model can be implemented for describing the leaching behavior of the three key Ca-compounds: $Ca(OH)_2$, $CaSO_4 \cdot 2H_2O$, and CaS.

The value of the equilibrium constant K_{eq3}, 1.11×10^{-7}, presented in Table 2 was calculated using the equilibrium concentration of pure CaS. The value reported here, together with Equation (17), can be used to develop utilization schemes for more complex OS ash-water systems that involve chemical reactions and also to treat similar alkaline waste materials.

3.3. Dissolution kinetics in OS ash-water systems

The dissolution kinetics of $Ca(OH)_2$ [34, 35] together with the mechanism of CaS dissolution [29, 31, 32, 36] has been described by several authors. In our previous studies [22, 37, 38], the main characteristics of the Ca dissolution process for OS ash were established on the basis of mass transfer mechanisms. In the current study, the leaching behavior of the main components in OS mineral wastes was investigated using the reaction kinetics approach.

Both the kinetic calculations and dissolution process simulations were performed using the MODEST 6.1 software package [39]. The software consists of a FORTRAN 95/90 library of objective functions, solvers and optimizers linked to model problem-dependent routines and the objective function. Each system of differential equations was solved by the means of linear multi-step methods implemented in ODESSA (a systematized collection of the ordinary differential equations solver), which is based on LSODE (Livermore Solver for Ordinary Differential Equations) software [40].

Using the dissolution model (Eqs. (1)–(7)), the dynamic concentration profiles of the characteristic species that participate in the OSA dissolution process can be modeled employing the differential equations presented below:

$$\frac{d[\text{CaS}]}{dt} = -k_{11}[\text{CaS}] + \frac{k_{11}}{K_1}[\text{CaS}][\text{Ca}^{2+}][\text{S}^{2-}]. \tag{9}$$

$$\frac{d[\text{Ca}^{2+}]}{dt} = k_{11}[\text{CaS}] - \frac{k_{11}}{K_1}[\text{CaS}][\text{Ca}^{2+}][\text{S}^{2-}] + k_{61}[\text{Ca(OH)}_2]$$
$$- \frac{k_{61}}{K_6}[\text{Ca(OH)}_2][\text{Ca}^{2+}][\text{OH}^-]^2 + k_{71}[\text{CaSO}_4] - \frac{k_{71}}{K_7}[\text{CaSO}_4][\text{Ca}^{2+}][\text{SO}_4^{2-}]. \tag{10}$$

$$\frac{d[\text{OH}^-]}{dt} = k_{21}[\text{S}^{2-}] - \frac{k_{21}}{K_2}[\text{OH}^-][\text{HS}^-] + k_{31}[\text{HS}^-] - \frac{k_{31}}{K_3}[\text{OH}^-][\text{H}_2\text{S}]$$
$$+ 2k_{61}[\text{Ca(OH)}_2] - \frac{k_{61}}{K_6}[\text{Ca(OH)}_2][\text{Ca}^{2+}][\text{OH}^-]^2. \tag{11}$$

$$\frac{d[\text{HS}^-]}{dt} = k_{41}[\text{HS}^-] - k_{51}[\text{HS}^-] + k_{21}[\text{S}^{2-}] - \frac{k_{21}}{K_2}[\text{HS}^-][\text{OH}^-] - k_{31}[\text{HS}^-]$$
$$+ \frac{k_{31}}{K_3}[\text{OH}^-][\text{H}_2\text{S}]. \tag{12}$$

$$\frac{d[\text{S}_2\text{O}_3^{2-}]}{dt} = 0.5k_{41}[\text{HS}^-]. \tag{13}$$

$$\frac{d[\text{SO}_4^{2-}]}{dt} = k_{51}[\text{HS}^-] + k_{71}[\text{CaSO}_4] - \frac{k_{71}}{K_7}[\text{CaSO}_4][\text{Ca}^{2+}][\text{SO}_4^{2-}]. \tag{14}$$

$$\frac{d[\text{S}^{2-}]}{dt} = k_{11}[\text{CaS}] - \frac{k_{11}}{K_1}[\text{CaS}][\text{Ca}^{2+}][\text{S}^{2-}] - k_{21}[\text{S}^{2-}] + \frac{k_{21}}{K_2}[\text{HS}^-][\text{OH}^-]. \tag{15}$$

$$\frac{d[\text{Ca(OH)}_2]}{dt} = -k_{61}[\text{Ca(OH)}_2] + \frac{k_{61}}{K_6}[\text{Ca(OH)}_2][\text{Ca}^{2+}][\text{OH}^-]^2. \tag{16}$$

$$\frac{d[\text{CaSO}_4]}{dt} = -k_{71}[\text{CaSO}_4] + \frac{k_{71}}{K_7}[\text{CaSO}_4][\text{Ca}^{2+}][\text{SO}_4^{2-}]. \tag{17}$$

The values of the reverse reaction rate constants (k_{x2}, $x = 1$–3, 6–7) may be expressed through the equilibrium constants as k_{x1}/K_x, $x = 1$–3, 6–7, accordingly. The concentrations in Equations (9)–(17) are expressed in

molar units. The concentration of H$^+$ ions can be found from the concentration of hydroxide ions ($[H^+] = K_w/[OH^-]$) or by using the pH ($[H^+] = 10^{-pH}$).

The reaction rate constants used in Equations (9)–(17) were estimated in the modeling of OS ash-water dissolution processes (the reaction rate constants k_{11}–k_{51} were used in all systems and were based on the pure CaS system). The estimated values of the rate constants k_{41} (2.01×10^{-4} s^{-1}) and k_{51} (8.66×10^{-5} s^{-1}) were one order of magnitude higher than the results reported by Mölder et al. [36] who investigated the rate of hydrolysis and oxidation (saturating the suspension with air) of CaS in a hydraulic ash disposal system. They reported rate constants for reactions (4) and (5) to be about 1×10^{-5} s^{-1} and approximately 4×10^{-6} s^{-1}, respectively. The reaction rate constants k_{61} and k_{71} at S/L ratios ranging from 0.004 to 0.2 were determined using the parameter estimation procedure that iteratively solved the proposed model equations and minimized the difference between these predictions and data obtained in batch experiments. For all data sets the correlation coefficient was greater than 0.87. The correlation coefficient of undersaturated model systems differed most from that of other model systems. In case of OS ash-water and ternary systems, k_{61} for the PF ash-water system and k_{71} for the SHC ash-water system agreed best.

As the next step, the simulation procedure was performed using the average values of rate constants (Table 3).

The accuracy of the proposed dissolution model ($R^2 > 90\%$) was confirmed by comparing the results of process simulations with experimental data. The concentration profiles, pH (Fig. 5), and the relative concentration of species for the OS ash-water and ternary model systems (S/L 0.004 and 0.1) resulting from modeling are shown in Figure 6.

The pH profile of the CFB ash-water model system follows the trend of the PF ash-water model system, the Ca(OH)$_2$ dissolution (Eq. 6) gives the highest alkaline reaction. In the SHC ternary system, the values of pH are

Table 3. Reaction rate constants for the systems under study

Reaction rate constant, s^{-1} / System		Average	
		Ash	Ternary
In all systems	k_{11}	0.00149	
	k_{21}	2.7700	
	k_{31}	8.4874	
	k_{41}	0.000201	
	k_{51}	0.0000866	
CFB	k_{61}	0.0171	0.0326
	k_{71}	0.0072	0.0214
PF	k_{61}	0.0294	0.0232
	k_{71}	0.0029	0.0175
SHC	k_{61}	0.0091	0.0340
	k_{71}	0.0266	0.0330
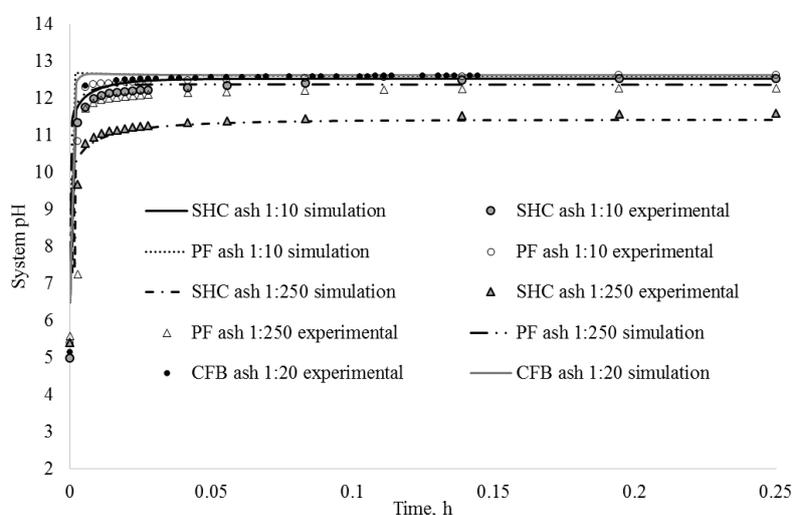
Fig. 5. Modeling of OSA dissolution: experimental vs simulated system pH.

higher (comparing $Ca(OH)_2$ contents in CFB and PF systems) due to the proton capture of sulfides, releasing the OH^- ions into the solution (Eqs. (2) and (3)).

The experimental results and simulated data in Figure 5 show that the pH of the system depends on the amount of the solid phase added because a greater amount of OS ash generates a faster increase in pH. The rate at which the equilibrium pH was reached differed between the selected ashes: it was slower for the real SHC ash system while the real PF ash system reached equilibrium more rapidly (Fig. 5). This implies that PF ash contains more compounds (Ca and Mg oxides) which ensure (dissolution of their hydrated forms) a fast basic reaction. This can also be seen from the reaction rate constants reported in Table 3, the value of the reaction rate constant for Equation (6) for the one-step (0.0282 s^{-1}) pure $Ca(OH)_2$ dissolution model [41] matches with the rate constant (0.0294 s^{-1}) for the PF ash system. The best accordance between OSA and ternary systems was achieved for k_{61} for the PF ash-water system and for k_{71} for the SHC ash-water system.

The experimental and model-predicted results for the pH and main ion concentrations agreed very well in the S/L ratio range of 1:10 to 1:250.

Plots of experimental and simulated concentration profiles for various S/L ratios for the PF ash-water system are presented in Figure 6. The sulfide content of SHC ash is two orders of magnitude higher than that of other ashes.

With regard to the calcium, sulfate and sulfide ions, the experimental results for the OS ash-water systems agree with simulated profiles. The PF ash-water system becomes saturated with calcium more rapidly than the others (Fig. 6a) because it has the highest content of CaO_{free} (22.37 wt%). The dissolution profiles of sulfate are rather similar in both the PF and CFB
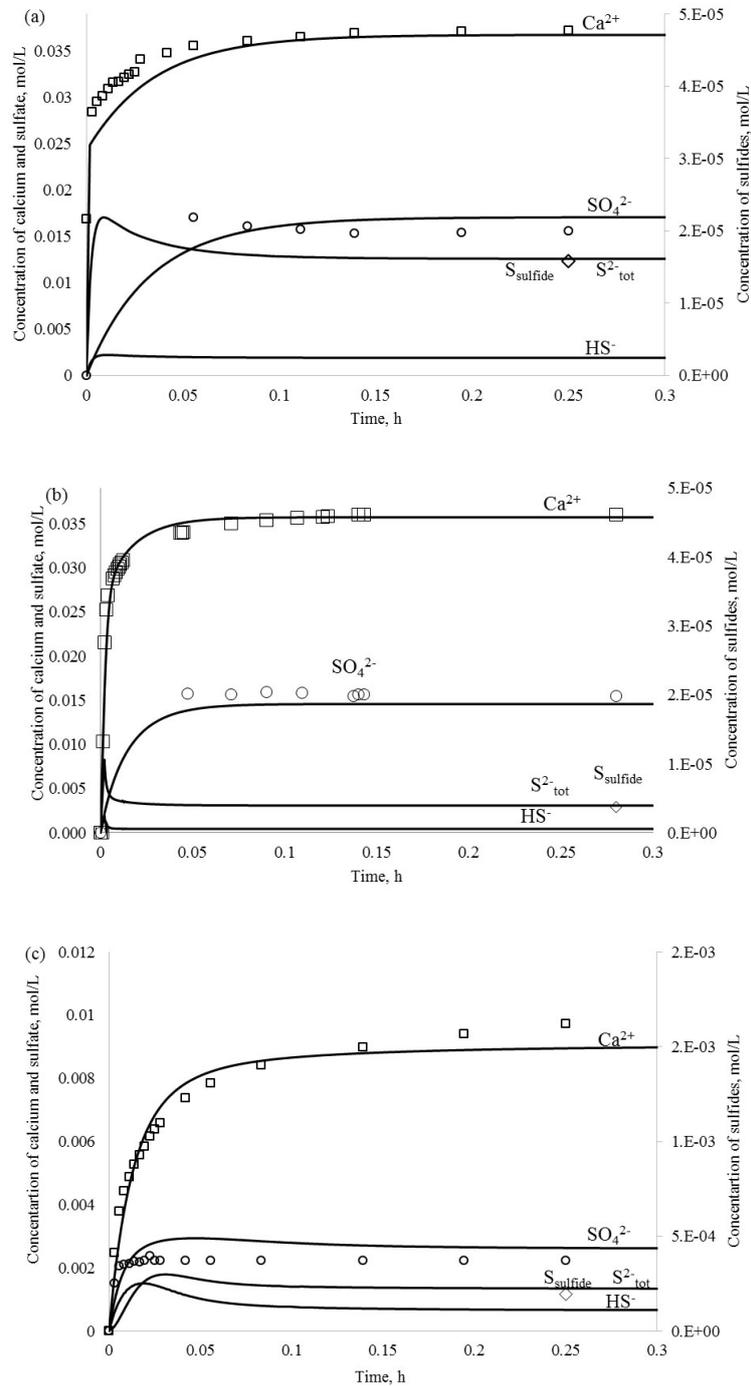
Fig. 6. Experimental vs MODEST 6.1 simulated leaching dynamics of key components of OSA from: (a) PF − S/L 1:10; (b) CFB − S/L 1:20; (c) SHC − S/L 1:50). (tot = total).

ash systems (Figs. 6a and 6b, respectively). However, due to the higher content of initial $CaSO_4$ (10.10 wt%) in raw CFB ash, the CFB ash-water system becomes saturated with sulfate more rapidly, as seen from the reaction rate constant k_{71} presented in Table 3. Regarding the SHC ash-water system, sulfate reaches equilibrium most rapidly, which is due to the oxidation of sulfides (Eq. (5)) present in a relatively high amount. The dissolution profiles of sulfides are related to the content of sulfides in the initial ash. The greater the amount of initial CaS added to the water system, the greater the concentration of sulfides in the liquid phase.

4. Conclusions

The leaching behavior of the main Ca-compounds in OS ash-water systems, which can be viewed as sorbents for both CO_2 mineralization and PCC production, were studied in order to provide a better understanding of the behavior of OS ash suspensions and leachates especially by wet deposition.

Based on the comparative equilibrium 3 h batch experiments, the thermo-dynamic results for the aqueous systems of three different types of OSAs (CFB, PF and SHC) as well as the corresponding model systems were obtained.

The results indicate that the provided OS ash leaching model simulations were in good agreement with experimental data, confirming its accuracy. The measured values of pH, conductivity, and the concentration of Ca^{2+} ions of OS ash-water systems were slightly higher than those of ternary model systems because the real OS ash contains other water-soluble components.

The authors also determined, according to the 3 h equilibrium concentrations, the thermodynamic equilibrium constants K_{eq1}–K_{eq3} and K_{eq6}–K_{eq7} for the dissolution reactions of $Ca(OH)_2$, $CaSO_4 \cdot 2H_2O$ and CaS in OS ash-water systems and proposed an empirical equation to calculate the concentration of Ca^{2+} ions as the dominating cation in OS ash leachates from conductivity measurements.

Furthermore, a kinetic reaction model, which incorporates dissolution mechanisms of $Ca(OH)_2$, $CaSO_4 \cdot 2H_2O$ and CaS, was constructed to describe OS ash-water systems.

Although the three types of OS ashes studied differ in chemical and physical structure, it was found that a single model provided results that were in good agreement with experimental data, and can therefore be used to describe the leaching behavior of the key Ca-compounds in OS ash.

The equilibrium constants determined can be used, firstly, to estimate the kinetics of dissolution and create a complete OS ash-water leaching model and, secondly, to design a pilot-scale OS ash-water carbonation reactor. The latter could significantly reduce the environmental impact of using oil shale and other Ca-rich fossil fuels in the energy sector.

The model constructed for the OS ash-water systems incorporates mechanisms of dissolution of $Ca(OH)_2$, $CaSO_4 \cdot 2H_2O$ and CaS. This model can be used to simulate all three types of OS ash (CFB, PF and SHC), which notably differ in chemical and physical structure. The proposed model and estimated parameters are thus suitable for describing the leaching of various types of ash that originate from the oil shale industry.

Acknowledgements

REFERENCES

1. Ots, A. Oil Shale Fuel Combustion. Tallinna Raamatutrükikoda, Tallinn, 2006.
2. Bauert, H., Kattai, V. Kukersite oil shale. In: *Geology and Mineral Resources of Estonia (Raukas, A., Teedumäe, A., eds.).* Estonian Academy Publishers, Tallinn, 1997, 313–327.
3. Kuusik, R., Uibu, M., Kirsimäe, K. Characterization of oil shale ashes formed at industrial-scale CFBC boilers. *Oil Shale*, 2005, **22**(4S), 407–419.
4. Bityukova, L., Mõtlep, R., Kirsimäe, K. Composition of oil shale ashes from pulverized firing and circulating fluidized-bed boiler in Narva Thermal Power Plants, Estonia. *Oil Shale*, 2010, **27**(4), 339–353.
5. Kuusik, R., Uibu, M., Kirsimäe, K., Mõtlep, R., Meriste, T. Open-air deposition of Estonian oil shale ash: formation, state of art, problems and prospects for the abatement of environmental impact. *Oil Shale*, 2012, **29**(4), 376–403.
6. Kattai, V., Saadre, T., Savitski, L. *Estonian Oil Shale: Geology, Resource, Mining Conditions*. Geological Survey of Estonia, Tallinn, 2000, 226 pp (in Estonian).
7. Golubev, N. Solid oil shale heat carrier technology for oil shale retorting. *Oil Shale*, 2003, **20**(3S), 324–332.
8. Reinik, J., Irha, N., Steinnes, E., Piirisalu, E., Aruoja, V., Schultz, E., Leppänen, M. Characterization of water extracts of oil shale retorting residues form gaseous and solid heat carrier processes. *Fuel Process. Technol.*, 2015, **131**, 443–451.
9. Talviste, P., Sedman, A., Mõtlep, R., Kirsimäe, K. Self-cementing properties of oil shale solid heat carrier retorting residue. *Waste Manage. Res.*, 2013, **31**(6), 641-647.
10. *Eesti Energia Annual Report 2014*. https://www.energia.ee/-/doc/10187/pdf/concern/annual_report_2014_eng.pdf (accessed in August 2015).
11. *VKG Yearbook 2014. Viru Keemia Grupp*. http://www.vkg.ee/cms-data/upload/juhatus/vkg-aastaraamat-eng-2014.pdf (accessed in August 2015).

12. *VKG Yearbook 2013. Viru Keemia Grupp.* http://www.vkg.ee/cms-data/upload/juhatus/vkg-aastaraamat-eng-2013.pdf (accessed in August 2015).

13. Uibu, M., Uus, M., Kuusik, R. CO_2 mineral sequestration in oil-shale wastes from Estonian power production. *J. Environ. Manage.*, 2009, **90**(2), 1253–1260.

14. Sanna, A., Uibu, M., Caramanna, G., Kuusik, R., Maroto-Valer, M. M. A review of mineral carbonation technologies to sequester CO_2. *Chem. Soc. Rev.*, 2014, **43**, 8049-8080.

15. Velts, O., Uibu, M., Kallas, J., Kuusik, R. Waste oil shale ash as a novel source of calcium for precipitated calcium carbonate: carbonation mechanism, modeling, and product characterization. *J. Hazard. Mater.*, 2011, **195**, 139–146.

16. Velts, O., Uibu, M., Kallas, J., Kuusik, R. CO_2 mineralisation: concept for co-utilization of oil shale energetics waste streams in $CaCO_3$ production. *Energy Procedia*, 2013, **37**, 5912–5928.

17. Reispere, H. J., Determination of free CaO content in oil shale ash. *Transact. Tallinn Polytechnical Institute*, series A, 1966, No 245, 73–76 (in Estonian).

18. EVS 664:1995. *Solid Fuels. Sulphur content. Determination of total sulphur and its bonding forms*.

19. APHA - American Public Health Association, American Water Works Association, Water Environment Federation. *Standard methods for examination of water and wastewater*, 21st ed., Washington DC, USA, 2005, 1368.

20. Külaots, I., Goldfarb, J., L., Suuberg, E., M. Characterization of Chinese, American and Estonian oil shale semicokes and their sorptive potential. *Fuel*, 2010, **89**, 3300-3306.

21. Tamm, K., Kuusik, R., Uibu, M., Kallas, J. Transformations of sulfides during aqueous carbonation of oil shale ash. *Energy Procedia*, 2013, **37**, 5905–5912.

22. Velts, O., Uibu, M., Rudjak, I., Kallas, J., Kuusik, R. Utilization of oil shale ash to prepare PCC: Leachability dynamics and equilibrium in the ash-water system. *Energy Procedia*, 2009, **1**(1), 4843–4850.

23. ISO-6058:1984. *Water quality – Determination of calcium content – EDTA titrimetric method*.

24. EKUK Virumaa Affiliate Kohta-Järve Laboratory of Chemistry. *The quality procedure guide TJ 17 – Determination of sulfide in water*, 2002.

25. ISO-9963-1:1994. *Water quality – Determination of alkalinity – Part 1: Determination of total and composite alkalinity*.

26. Ritchie, I. M., Bing-An, X. The kinetics of lime slaking. *Hydrometallurgy*, 1990, **23**(2-3), 377–396.

27. Sun, W., Nešić, S., Young, D., Woollam, R. C. Equilibrium expressions related to the solubility of the sour corrosion product mackinawite. *Ind. Eng. Chem. Res.*, 2008, **47**(5), 1738–1742.

28. Almgren, T., Dyrssen, D., Elgquist, B., Johansson, O. Dissociation of hydrogen sulphide in seawater and comparison of pH scales. *Mar. Chem.*, 1976, **4**(3), 289–297.

29. Tamm, K., Uibu, M., Kallas, J., Kallaste, P., Velts-Jänes, O., Kuusik, R. Thermodynamic and kinetic study of CaS in aqueous systems. *Fuel Process. Technol.*, 2016, **142**, 242–249.

30. Irha, N., Uibu, M., Jefimova, J., Raado, L.-M., Hain T., Kuusik, R., Leaching behaviour of Estonian oil shale ash-based construction mortars. *Oil Shale*, 2014, **31**(4), 394–411.

31. Tamm, K., Kuusik, R., Uibu, M., Kallas, J. Transformations of sulfur compounds in oil shale ash suspension. In: *Waste Management and the Environment*

VI: 6th International Conference on Waste Management and the Environment, New Forest, UK, 04.–06.07.2012 (Popov, V., Itoh, H., Brebbia, C. A., eds.). Wessex Institute of Technology Press, (WIT Transactions on Ecology and the Environment), 2012, 163.

32. Tamm, K., Kuusik, R., Uibu, M., Kallas, J. Behaviour of sulfur compounds during aqueous leaching of oil shale ash. In: *Proc. 4th Int. Conf. on Accelerated Carbonation for Environmental and Materials Engineering ACEME 2013*, Leuven, Belgium, 9–12 April 2013 (Nasser, R., Santos, R., Cizer, Ö., Van Gerven, T., eds.). Leuven, 2013, 541–544.

33. Aavik, J. Characterization of oil shale ash leachate for optimizing the precipitation of calcium carbonate. Master's Degree, Tallinn University of Technology, 2011 (in Estonian).

34. Johannsen, K., Rademacher, S. Modelling the kinetics of calcium hydroxide dissolution in water. *Acta Hydroch. Hydrob.*, 1999, **27**(2), 72–78.

35. Giles, D. E., Ritchie, I. M., Xu, B.-A. The kinetics of dissolution of slaked lime. *Hydrometallurgy*, 1993, **32**(1), 119–128.

36. Mölder, L., Elenurm, A., Tamvelius, H. Sulphur compounds in a hydraulic ash-disposal system. *Proc. Estonian Acad. Sci. Chem.*, 1995, **44**(2/3), 207–211.

37. Velts, O., Hautaniemi, M., Kallas, J., Kuusik, R. Modeling calcium dissolution from oil shale ash: Part 1. Ca dissolution during ash washing in a batch reactor. *Fuel Process. Technol.*, 2010, **91**(5), 486–490.

38. Velts, O., Hautaniemi, M., Kallas, J., Kuosa, M, Kuusik, R. Modeling calcium dissolution from oil shale ash: Part 2. Continuous washing of the ash layer. *Fuel Process. Technol.*, 2010, **91**(5), 491–495.

39. Haario, H. *Modest User's Manual*. Profmath OY, Helsinki, Finland, 1994.

40. Hindmarsh, A. C. ODEPACK, a systematized collection of ODE solvers. In: *Scientific Computing: IMACS Transactions on Scientific Computation* (Stepleman, R. S. et al., eds.), North-Holland, Amsterdam, 1983, **1**, 55–64.

41. Uibu, M., Tamm, K., Velts-Jänes, O., Kallaste, P., Kuusik, R., Kallas, J. Utilization of oil shale combustion wastes for PCC production: Quantifying the kinetics of $Ca(OH)_2$ and $CaSO_4 \cdot 2H_2O$ dissolution in aqueous systems. *Fuel Process. Technol.*, 2015, **140**, 156–164.